Int J Physiol Pathophysiol Pharmacol 2012;4(3):115-127
www.ijppp.org /ISSN:1944-8171/IJPPP1208006

Original Article

Dimebon alters hippocampal amyloid pathology in 3xTg-AD mice

Sylvia E Perez[1], Muhammad Nadeem[1], Katherine R Sadleir[2], Joanna Matras[1], Christy M Kelley[1], Scott E Counts[1], Robert Vassar[2], Elliott J Mufson[1]

[1]Department of Neurological Sciences, Rush University Medical Center, Chicago, IL 60612; [2]Department of Cell and Molecular Biology, Feinberg School of Medicine, Northwestern University, Chicago, IL 60611

Received August 28, 2012; accepted September 17, 2012; Epub September 20, 2012; Published September 30, 2012

Abstract: A double blind, placebo-controlled phase II study revealed that the antihistamine, Dimebon® (dimebolin, latrepirdine) improved cognition in Alzheimer disease (AD) patients compared to placebo controls. However, the Phase III CONNECTION trial failed to demonstrate significant differences between dimebon and placebo treatments. Despite the controversial therapeutic outcomes in the treatment of AD, dimebon's mechanism(s) of action within the brain remain unclear. In the present study, we evaluated the effects of dimebon upon β-amyloid (Aβ), tau and astrocytes in the hippocampus of triple transgenic (3xTg-AD) mice, which develop AD-like pathology in an age-dependent manner. At age 6.5 months, prior to the development of Aβ plaques in the hippocampus, male and female 3xTg-AD mice, received a daily intraperitoneal injection of 0.1 % dimebon or saline for 1.5 months. At 8 months, quantitative immunohistochemistry revealed a significant reduction in hippocampal/subicular APP/Aβ in dimebon-treated mice, whereas protein bioassay found no change in full length APP, soluble $A\beta_{1\text{-}40}$ and $A\beta_{1\text{-}42}$, Aβ oligomers, BACE1 and GFAP levels between groups. Interestingly, the number of the hippocampal APP/Aβ plaques in female and male dimebon-treated mice was higher compared to gender-matched control mice. Dimebon did not alter hippocampal tau levels. Furthermore, dimebon protects SH-SY5Y neurons against Aβ toxicity and promotes GFAP expression in primary mouse astrocyte cultures. Our findings demonstrate that dimebon *in vivo* modifies hippocampal APP/Aβ pathology and *in vitro* protects against Aβ toxicity promoting cell survival and activates astrocytes.

Keywords: Alzheimer's disease, amyloid, dimebon, hippocampus, plaques, tangles, tau, transgenic mice

Introduction

Dimebon or dimebolin (latrepirdine: 2,3,4,5-Tetrahydro-2, 8-dimethyl-5-(2-6(6-methyl-3-pyridyl)ethyl)-1H-pyrido(4,3-b) indole), an unspecific antihistamine, was initially shown in clinical trials to improve cognition in patients with mild to moderate Alzheimer's disease (AD) [1, 2] and Huntington's (HD) [3]. However, a recent multinational double-blinded Phase III study (CONNECTION) failed to demonstrate differences in cognition between dimebon and placebo treated subjects with mild to moderate AD [4]. Notably, preclinical studies in rodents [1, 5, 6], Tg CRND8 AD mice [7] and monkeys [8] revealed that dimebon enhances hippocampal-related memory function. However, the mechanism of action underlying these beneficial effects for hippocampal function is unclear. In the present study, we evaluated the effect that dimebon pretreatment has upon hippocampal neuropathology in a triple transgenic mouse model of AD (3xTg-AD) [9, 10]. These mice display extensive hippocampal Aβ plaque and intraneuronal tau inclusions [9-11] similar to that seen in AD [12-14] together with hippocampal-dependent memory impairment [9]. In addition, these mice also feature astrocytosis in close apposition to Aβ plaques in the hippocampus, mimicking that seen in AD [15]. Hence, we examined whether dimebon influenced amyloid plaque and tau pathology as well as astrocytosis in 3xTg-AD mice. In addition, we also examined the effects of dimebon upon neurons and astro-

Table 1. Demographics and treatment characteristics

Genotype	Treatment (i.p.)	n	gender	Age at start	Sacrifice age	
3×Tg-AD	Dimebon 1 mg/kg	5	female	6.5 mo	8 mo	45 days treatment
		6	male	6.5 mo	8 mo	
	Saline 0.9% NaCl	3	female	6.5 mo	8 mo	
		4	male	6.5 mo	8 mo	

cytes *in vitro*.

Materials and methods

Subjects and tissue collection

Six-and-a-half month-old male (n=10) and female (n=8) 3xTg-AD mice from our in-house colony received either a daily intraperitoneal (i.p.) injection of dimebon (1 mg/kg; Sinochemexper, China) or saline (0.9% NaCl) for 45 days (**Table 1**). These mice were generated in a hybrid 129/C57BL/6 background carrying the human mutated Swedish amyloid precursor protein mutation (APP_{swe}), presenilin 1 ($PS1_{M146V}$) and Tau_{P301L} genes [9]. Subjects were given *ad libitum* access to standard rodent chow and water and maintained on a 12h:12h light:dark cycle. Mice were randomized to each experimental group (**Table 1**). All animal care and procedures were conducted with approved institutional animal care protocols and in accordance with the NIH Guide for the Care and use of Laboratory Animals.

Twenty-four hours after the last injection and under deep anesthesia (ketamine 95mg/kg and xylazine 5mg/kg) mice were transcardially perfused with cold 0.9% saline. All brains were rapidly removed from the calvarium and hemisected on wet-ice. One hemisphere was immersion-fixed in a solution containing 4% paraformaldehyde/0.1 % glutaraldehyde in 0.1 M phosphate-buffered saline (PBS; pH 7.4) for 24 hours at 4°C, cryoprotected in a phosphate buffer (PB) solution containing 30% sucrose for 24 h at 4°C, sectioned frozen on a sliding knife microtome in the coronal plane at 40-micron thickness into six adjacent series and the sections stored at -20°C in a cryoprotectant solution (30 % ethylene glycol, 30 % glycerol, in 0.1 M PBS). The other hemisphere was cut into 1 mm coronal slabs on wet-ice in a stainless steel brain blocker and hippocampi were dissected using fiduciary landmarks and quickly frozen on dry ice and stored at -80°C as previously described [16].

Liquid Chromatography-tandem mass spectrometry (LC-MS/MS)

The initial structural and purity analysis of dimebon (Sinochemexper Company, China) was performed with a Shimadzu IT-TOF mass spectrometer equipped with a Shimadzu Prominence High-Performance Liquid Chromatography (HPLC) system (Shimadzu Scientific Instruments, Columbia, MD) as described by Nirogi et al. [17]. Dimebon was resolved through a 2.1x100mm Hypersil Gold reverse phase column (ThermoFisher, Walthman, MA, USA) and eluted with 50 % methanol (v/v) with 0.1 % formic acid mobile phase. Dimebon was scanned in a range of 200-2000 m/z in both positive and negative modes. The source temperature was set at 350°C and the ESI voltage set to 4.4 kV. Collision energy range was set to 30 eV to observe the 320→277 transition, using a scan width of 2.0 atomic mass units and a scan time of 150 ms for each compound. Spectrometric data was collected and analyzed. Based on this 320→277 transition, our mass spectral findings indicated that the purity of dimebon is greater than 99%.

Dimebon was measured 45 days post treatment using LC-MS/MS in brain tissue harvested from 3xTg-AD mice. Brainstem samples were weighed and three volumes of the internal standard solution (IS; 100 pg *N*-$^{13}CD_3$-Dimebon in 100 ml of methanol) were added. For standard curve and quality control, blank rat brain was weighted and three volumes of standard solution containing dimebon concentrations ranging from 10 to 10,000 pg/ml were added. All samples were homogenized at 4 m/s for 45 seconds on a FastPrep ^{R}-24 (MP Biomedicals; Biocampare, South San Francisco, CA) followed by centrifugation at 3,200 rcf for 15 min. Supernatant (100 µL) was added to 100 µl of water and centrifuged at 16,000 rcf for 10 min. HPLC was performed using a CTC Leap autosampler

with a Variant Pursuit PFP (50 x 2.0 mm, 3 µl) column at ambient temperature. Samples were eluted by the use of a gradient mobile phase consisting of A (100 mM ammonium formate in water with 0.02% formic acid) and B (0.1% formic acid in methanol:acetonitrile (9:1)). The initial mobile phase composition of 5% B was followed by a linear gradient at the time of injection to 50% B at 3 min. This was followed by a second linear gradient to 98% B at 5 min which was held for 0.2 min before re-equilibration to 5% B. The phase mobile was pumped at a total flow rate of 0.6 ml/min. Mass spectrometry detection was performed with the triple quadruple spectrometer API 5000 (Applied Biosystems/MDS SCIEX, Foster City). The turbo ion spray (ESI) interface was operated in positive mode and monitored for detection of dimebon at 320.2 m/z to 277.2 m/z and for *N*-$^{13}CD_3$-Dimebon (IS) at 324.2 m/z to 277.2 m/z. Chromatographic and spectrometric data was collected and analyzed using Analyst 1.2.

Immunohistochemistry, densitometry, and plaque counts

Floating-sections were immunostained using antibodies directed against the amyloid precursor protein (APP)/amyloid beta (Aβ) or the tau conformational Alz50 isoform using the peroxidase avidin-biotin method to amplify the antigen signal. Sections were incubated with mouse monoclonal IgG-anti APP/Aβ (6E10, 1:2,000; Covance, NJ) and IgM-anti Alz50 (1:10,000; a gift from Professor Peter Davies, Albert Einstein College of Medicine, NY) overnight at room temperature, after incubation with the appropriate biotinylated secondary antibody (1:200, Vector Labs, CA), and amplification using the Vectastain ABC kit (Vector Labs, CA), immunoreactions were revealed using diaminobenzidine (DAB, Sigma, St Louis, IL) as previously described [11]. Immunocytochemical controls consisted of elimination of the primary antibodies resulting in lack of staining [11].

Optical density (OD) measurements of 6E10 and Alz50 immunoreactivity within the hippocampal subicular complex were determined with the aid of the Scion Image 1.60 program (Frederick, MD) as described previously [18, 19]. Briefly, every sixth section (separated by 240 µm) was analyzed using 40x and 10x objectives, centering the camera over the field of interest. The captured frame was manually outlined from an average of 5 to 7 sections for 6E10 and 2 sections for Alz50 from each animal to obtain OD measurements. The OD measurements were automatically analyzed in grey-scale images, using the computer program. Five ODs from regions of the hippocampus devoid of 6E10 and Alz50 immunostaining were measured, averaged, and subtracted from the final 6E10 and Alz50 OD values. Previous studies revealed that OD measurements reflect changes in protein expression, which parallel those obtained using a biochemical protein assay [18, 20]. In addition, the number of APP/Aβ positive plaques in the subiculum was manually counted in one entire hippocampal series of sections with the aid of a Nikon Eclipse 80i microscope using a 20x or 10x objective and 10x ocular magnification.

Western and dot blotting procedures

Frozen hippocampus was used to quantify the full-length amyloid precursor protein (APP), β-secretase 1 (BACE1, beta-site cleavage APP enzyme) and glial fibrillary acidic protein (GFAP, an intermediate filament of the astrocyte cytoskeleton). Samples were processed in Tris-buffered saline (TBS) with protease inhibitor mixture, homogenized and sonicated as described previously (Perez et al., 2010) [16]. The homogenate was centrifuged and the supernatant fraction (S1, soluble fraction) was collected and frozen at -80°C. Protein was determined by the Bradford method (Bio-Rad, Hercules, CA). To detect full length APP (105-110 kDa) and GFAP (50 kDa), 50 µg and 25 µg protein samples were separated in 7.5% SDS polyacrylamide gel electrophoresis (Lonza, Rockland, ME) respectively, and then transferred to polyvinylidene fluoride (PVDF) membranes (Immobilon P; Millipore, Bedford, MA). After blocking in TBS/0.1% Tween-20/5% milk for 30 min, independent western blots were incubated with 6E10 (1:1000; Covance, NJ) and GFAP (1:1000; DAKO, Carpinteria, CA) antibodies followed by horseradish peroxidase (HRP)-conjugated goat anti-mouse IgG (1:8,000; ThermoFisher, Walthman, MA) and HRP-conjugated goat anti-rabbit IgG (1:500; Pierce, Rockford, IL), respectively. To detect BACE1 samples were separated using Nu Page 4-12% Bis-Tris gel (Invitrogen, Carlsbad, CA) and transferred to PVDF membranes. Blots were incubated with mouse anti-BACE1 (3D5; provided by Dr. Robert Vassar, Northwestern University Medical School,

Chicago, IL) at 1:1000 and reacted with HRP-goat anti-mouse IgG (1:10,000; Jackson ImmunoResearch Laboratories, West Grove, PA). All blots were developed by chemiluminescence on a Kodak 1D Image Station 440CF (Perkin-Elmer, Wellesley, MA) and quantified by densitometry. β-actin (42 kDa, mouse anti-β-actin IgG, 1:30,000; Sigma, St. Louis, MO) and gyceraldehyde-3-phosphate dehydrogenase (GADPH) (37 kDa, rabbit anti-GADPH IgG, 1:500; Millipore Bedford, MA) were used as a loading control for APP and GFAP, respectively and β-tubulin for BACE1 (50 kDa, mouse anti-β-tubulin IgG, 1:10,000; Millipore, Bedford, MA). Western blots were done in triplicate and analyzed by an observer blinded to experimental conditions.

Dot blotting was used to quantify soluble hippocampal levels of $A\beta_{1-40}$ and $A\beta_{1-42}$, Aβ oligomers and tau conformational Alz50 and phosphorylational AT8 (Phosphoserine 202 and Phosphothreonine 205) tau isoforms, 1 μg of the soluble fraction was directly applied onto gridded nitrocellulose (Protran BA 85/20; Whatman, Miami, FL) in a final volume of 2 μl. Blots were air-dried, blocked for 1 h, and incubated overnight with Aβ1-40, Aβ1-42 (1:50; Invitrogen, Carlsbad, CA), A11 (1:5000 dilution; Millipore), Alz50 (1:5000), AT8 (1:1000; ThermoFisher, Walthman, MA) or β-actin (1:20,000, Sigma, MO) antibodies. The following day, after several rinses, blots were incubated for 1 h at room temperature with either HRP-conjugated goat anti-rabbit IgG secondary antibody (1:5000; Bio-Rad, Hercules, CA) or HRP-conjugated goat anti-mouse IgG (1:8,000; ThermoFisher, Walthman, MA) as appropriate. Immunoreactive proteins were visualized by enhanced chemiluminescence (Amersham Biosciences, Piscataway, NJ) on a Kodak 1D Image Station 440CF (Perkin-Elmer, Wellesley, MA) and quantified by densitometry using the Image J 1.43 program (NIH). This experiment was performed in triplicate.

Neuronal and astrocyte in vitro procedures

SH-SY5Y human neuroblastoma cultures were maintained in DMEM/10% fetal bovine serum and treated with 10 μM all-*trans* retinoic acid (Sigma, St. Louis, MO) for neuronotypic differentiation. To test whether dimebon is neuroprotective against Aβ, cultures were pretreated with a range of dimebon concentrations (10-50 μM) and then challenged with 10 μM $A\beta_{1-42}$, 10 μM $A\beta_{25-35,}$ or reverse peptide. $A\beta_{25-35}$ was dissolved in DMSO and applied without pre-aggregation, which results in the rapid formation of oligomeric and protofibril intermediates in aqueous solutions [21, 22]. $A\beta_{1-42}$ was dissolved in DMSO and pre-aggregated for 16 hours at 37° C. Western blotting revealed an accumulation of SDS-soluble immunoreactive material migrating at ~40-48 kDa reminiscent of oligomeric amyloid [23, 24] (data not shown). Neuronal viability was determined by propidium iodide uptake following 2 days of Aβ treatment [25].

Primary astrocytes were isolated from 2- to 5-day old mice as previously described [26, 27]. Briefly, cerebra were chopped, triturated, passed through mesh, and trypsinized for the isolation of mixed glial cells. On day 9, the mixed glial cultures were washed three times with DMEM/F-12 (Invitrogen, Carlsbad, CA) and shaken at 240 rpm for 2 h at 37°C on a rotary shaker to isolate microglia. Similarly, on day 11, cells were shaken at 180 rpm for 18 h to remove oligodendroglia. Then, the attached cells, primarily astrocytes, were subcultured onto poly-D-lysine coated 96-well plates or 8-well chamber slides. To test whether dimebon promotes astrocytic expression of GFAP, astroglia were treated with 10, 25 and 50 μm dimebon concentrations for 1, 2 and 3 days. After treatment astrocytes were fixed with 4 % paraformaldehyde/0.1 % glutaraldehyde for 30 min, rinsed in PB and TBS-TritonX-100 solution, then incubated with a rabbit antibody against to GFAP (1:200, DAKO, Carpinteria, CA) overnight and visualized with Cy3-donkey anti-rabbit Ig G (1:300, Jackson ImmunoResearch Laboratories) under an inverted Nikon Eclipse Ti microscope (Nikon Instruments Inc, IL). Quantification of immuofluorescence expression in astrocyte cultures was evaluated with a microplate reader SpectraMax M5 (Molecular Devices, Sunnyvale, CA).

Statistical analysis

Data obtained from LC-MS/MS, immunohistochemistry/densitometry, western blot, dot blot, plaque counts and cell cultures were evaluated using non-parametric Mann-Whitney rank-sum for two groups, and Kruskal-Wallis rank-sum for multiple groups followed by a *post hoc* test for pair-wise comparisons, as appropriate (Sigma Stat 3.5; Systat Software, Inc., San Jose, CA). Data were graphically represented using the

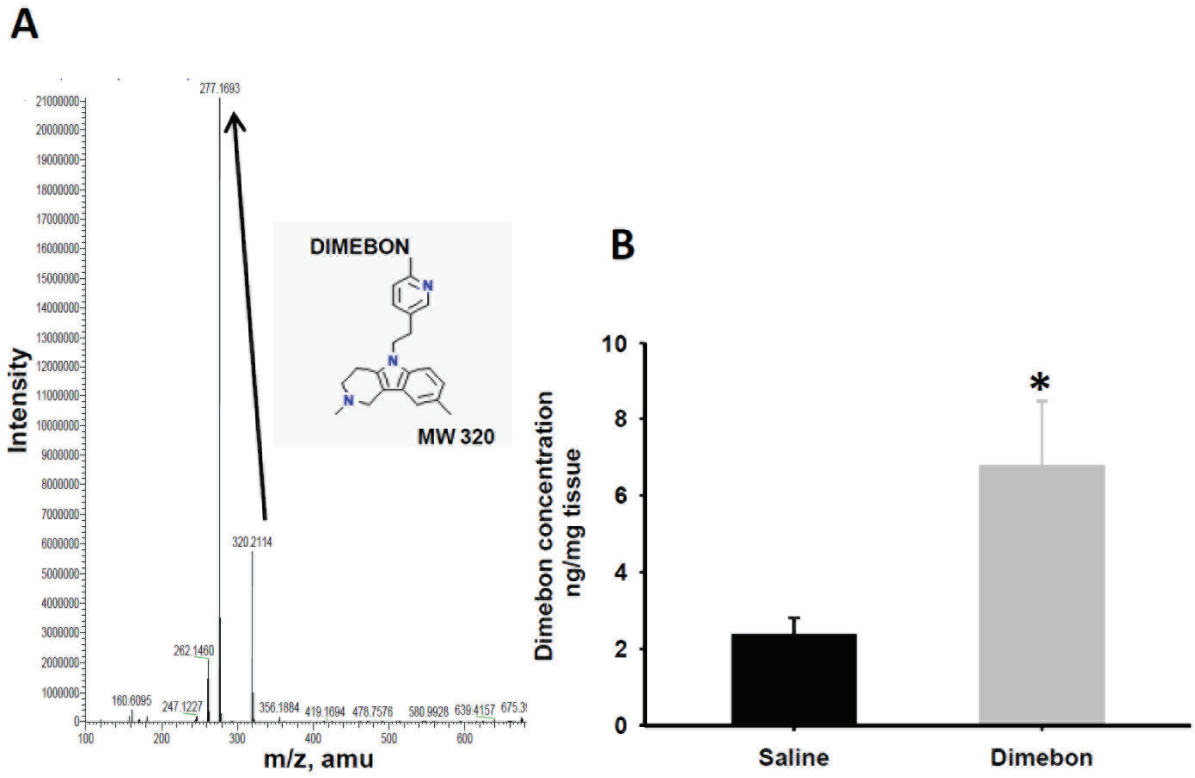

Figure 1. (A) Mass spectral graph showing the main derived product after ionization of dimebon at 277 m/z. (320 dimebon molecular weight (MW). (B) Histogram showing dimebon concentration mean values in the brainstem of 3xTg-AD mice treated with saline and dimebon. Statistical analysis revealed that the amount of brain dimebon was significantly higher than in saline-treated 3xTg-AD mice. (*p < 0.05).

means and standard error of the mean (SEM) (Sigma Plot 10.0; Systat Software, Inc., San Jose, CA). Correlations were performed with Spearman test. The level of statistical significance was set at 0.05 (two-sided).

Results

LC-MS/MS dimebon analysis

Mass spectral analysis revealed a pattern of fragmentation for dimebon (molecular weight 320) similar to previous reports [17], with a predicted parent peak at 320 m/z and a main product derived from ionization of dimebon at 277 m/z (**Figure 1A**). This later resulted from a loss of methyl-methylene-amine group of the dimebon molecule. These results confirm that the drug we injected into the mice is consistent with the chemical identity of dimebon. Moreover, the 320→277 transition indicated that the purity of the dimebon used in the present study is greater than 99% (**Figure 1A**).

LC-MS/MS was used to measure the amount of dimebon in the brain after 45 daily injections in 3xTg-AD mice. Saline-treated mice showed a mean value of 2.37 ng/mg of dimebon, which was interpreted as background level compared to an average of 6.78 ng/mg in the dimebon-treated mouse brain. Statistical analysis of the measurements obtained by LC-MS/MS revealed that dimebon levels were significantly higher in the drug-treated compared to saline-treated 3xTg-AD mice (**Figure 1B**; Mann-Whitney rank sum test, p=0.013).

Reduction in optical density (OD) measurements in dimebon-treated 3xTg-AD mice

Light-microscopic evaluation of 6E10 immunostaining revealed a striking reduction in neuropil and CA1 neuronal reactivity within the hippocampal subicular complex in dimebon com-

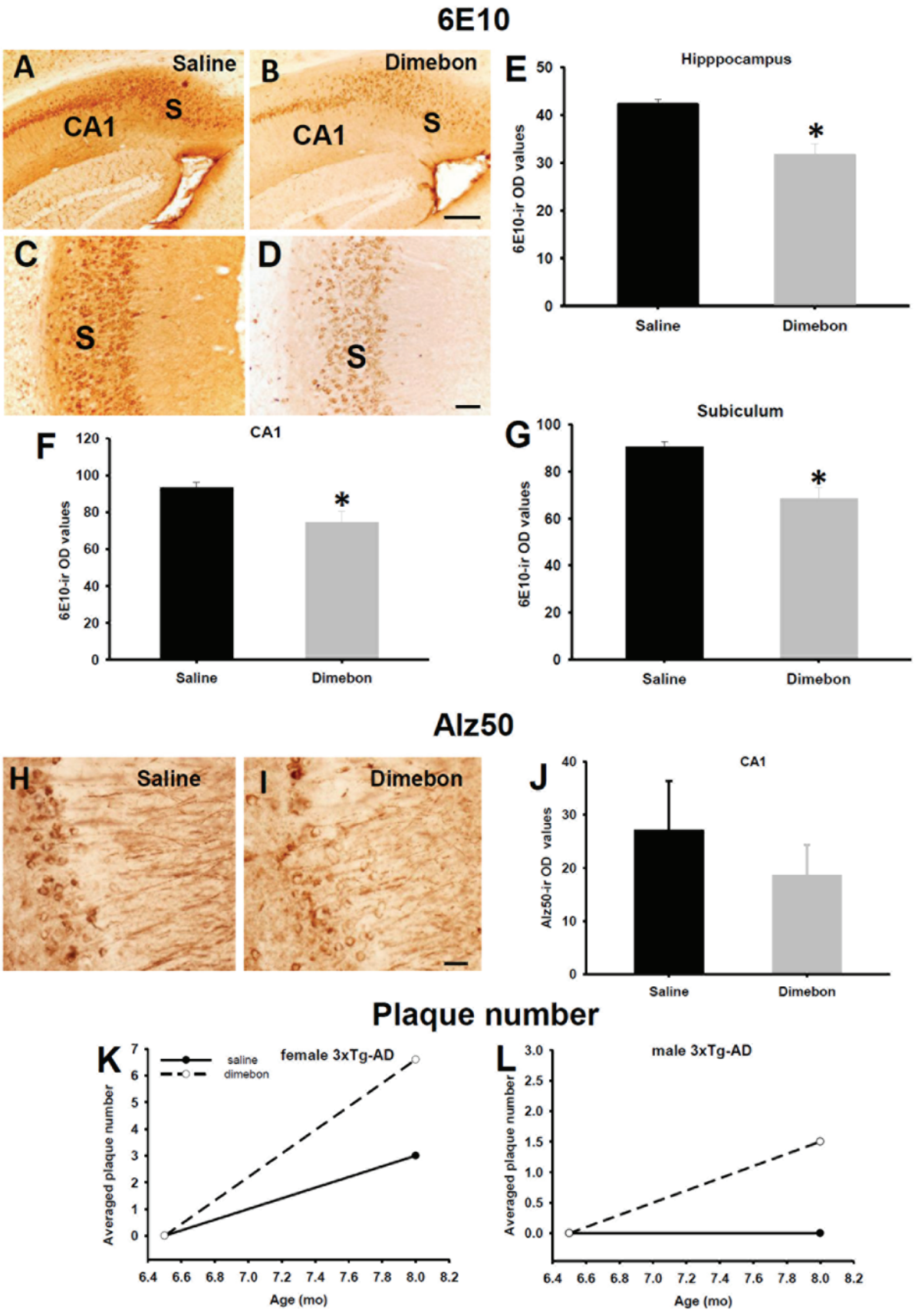
6E10
A
Saline
CA1
S
B
Dimebon
CA1
S
C
S
D
S
E
Hipppocampus
6E10-ir OD values
50
40
30
20
10
0
*
Saline
Dimebon
F
CA1
6E10-ir OD values
120
100
80
60
40
20
0
*
Saline
Dimebon
G
Subiculum
6E10-ir OD values
100
80
60
40
20
0
*
Saline
Dimebon
Alz50
H
Saline
I
Dimebon
J
CA1
Alz50-ir OD values
40
30
20
10
0
Saline
Dimebon
Plaque number
K
saline
dimebon
female 3xTg-AD
Averaged plaque number
7
6
5
4
3
2
1
0
6.4 6.6 6.8 7.0 7.2 7.4 7.6 7.8 8.0 8.2
Age (mo)
L
male 3xTg-AD
Averaged plaque number
3.0
2.5
2.0
1.5
1.0
0.5
0.0
6.4 6.6 6.8 7.0 7.2 7.4 7.6 7.8 8.0 8.2
Age (mo)

Figure 2. (A-D) Images of the hippocampal-subicular formation showing a major reduction in 6E10 (APP/Aβ) immunoreactivity in the hippocampal CA1 field and subiculum in a female dimebon-treated (B and D) compared to a female saline-treated 3xTg-AD mouse (A and C). This histological observation was statistical confirmed by densitometry where the reduction in 6E10-ir optical density (OD) measurements was significant in the entire hippocampal formation (E), CA1 pyramidal neurons (F) and pyramidal+neuropil in the subiculum (G) in dimebon compared to saline-treated 3xTg-AD mice. (H and I) Images illustrating minor reduction in Alz50 immunostaining in the CA1 field of the hippocampus in dimebon-treated (H) compared to saline-treated mouse (I). (J) Statistical analysis revealed no significant difference in Alz50-ir OD measurements between dimebon and saline-treated mice. Note that Alz50-ir OD measurements had a tendency to a decrease in dimebon-treated mice (p=0.057). (K and L) Plaque counts revealed a trend to increase in the averaged of 6E10 positive plaque numbers in female dimebon compared to female saline-treated 3xTg-AD mice (K), and the plaque averaged number in male treated mice was 1.5 (L), whereas no plaques were seen in male 3xTg-AD mice receiving only saline (L). Abbreviations: CA1, hippocampal CA1 field and S, subiculum. Scale bars: A,B=200 μM, C,D=100 μM and H,I=40 μM.

pared to saline-treated male and female 3xTg-AD mice (**Figure 2A-D**). OD measurements of the entire hippocampal formation (**Figure 2E**), CA1 pyramidal neurons (**Figure 2F**) or the neuropil+neurons in the subiculum (**Figure 2G**) revealed a significant reduction in 6E10 immunoreactivity in dimebon compared to saline treated 3xTgAD mice, independent of the gender (Mann-Whitney rank-sum test, $p<0.01$). In addition, dimebon concentrations were negatively correlated with subicular 6E10 OD measurements (Spearman correlation coefficient =-0.603, p=0.013).

The hippocampus showed a minor reduction in Alz50 immunoreactivity in CA1 neurons in dimebon compared to saline-treated 3xTg-AD mice (**Figure 2H** and **2I**). Statistical evaluation of Alz50 immunoreactive (-ir) OD measurements in CA1 pyramidal cells revealed a trend towards a decrease without reaching significance in dimebon compared to the saline-treated mice (**Figure 2J**; Mann-Whitney rank-sum test, p=0.057).

Plaque numbers in dimebon-treated 3xTg-AD mice

Plaque number was manually counted in one full series throughout the hippocampal complex stained with the 6E10 antibody. We found that dimebon or saline-treated mice displayed 6E10 positive plaques in the subiculum at 8 months of age in female 3xTg-AD mice. Although the averaged number of 6E10 positive plaques was 2 fold higher in the subiculum of female dimebon versus saline-treated mice, the difference was not significant (**Figure 2K**; Mann-Whitney rank sum test, $p>0.05$). Interestingly, an average of 1.5 6E10 positive plaques was found in the subiculum in dimebon injected, whereas no APP/Aβ plaques were seen in saline-treated male 3xTg-AD mice (**Figure 2L**).

Stable levels of APP, GFAP and BACE1 in dimebon-treated 3xTg-AD mice

The relative levels of full length APP, BACE1 and GFAP in the hippocampus of 3xTg-AD mice were examined after treatment by quantitative immunoblotting. Western-blot analysis revealed no differences in hippocampal APP or BACE protein levels between dimebon and saline-treated 3xTg-AD mice. In addition, GFAP protein levels were unchanged between the groups examined (**Figure 3**). Dot blot analysis did not reveal difference in levels of soluble $A\beta_{1-40}$, $A\beta_{1-42}$ and Aβ oligomers (A11) from hippocampal homogenates from dimebon or saline-treated 3xTg-AD mice (**Figure 4A-F**). Likewise, soluble levels of Alz50 and AT8 were unchanged between the examined groups (**Figure 4G-J**).

Dimebon prevents Aβ neuronal toxicity in vitro

To determine whether dimebon provided neuroprotection against amyloid toxicity *in vitro*, SH-SY5Y human neuronotypic cultures were pretreated with dimebon prior to challenge with either $A\beta_{1-42}$ or $A\beta_{25-35}$ (**Figure 5A** and **5B**). Whereas cell death was significantly increased in cultures exposed to $A\beta_{1-42}$ or $A\beta_{25-35}$ alone, pretreatment with 25μM or 50μM dimebon provided significant protection against amyloid-mediated neurotoxicity (**Figure 4A** and **4B**; Kruskal-Wallis on ranks $p<0.01$).

Dimebon increases GFAP expression in primary astrocyte mouse culture

To evaluate whether dimebon stimulates the production of GFAP *in vitro*, the intensity of GFAP immunofluorescence in astrocyte cell cul-

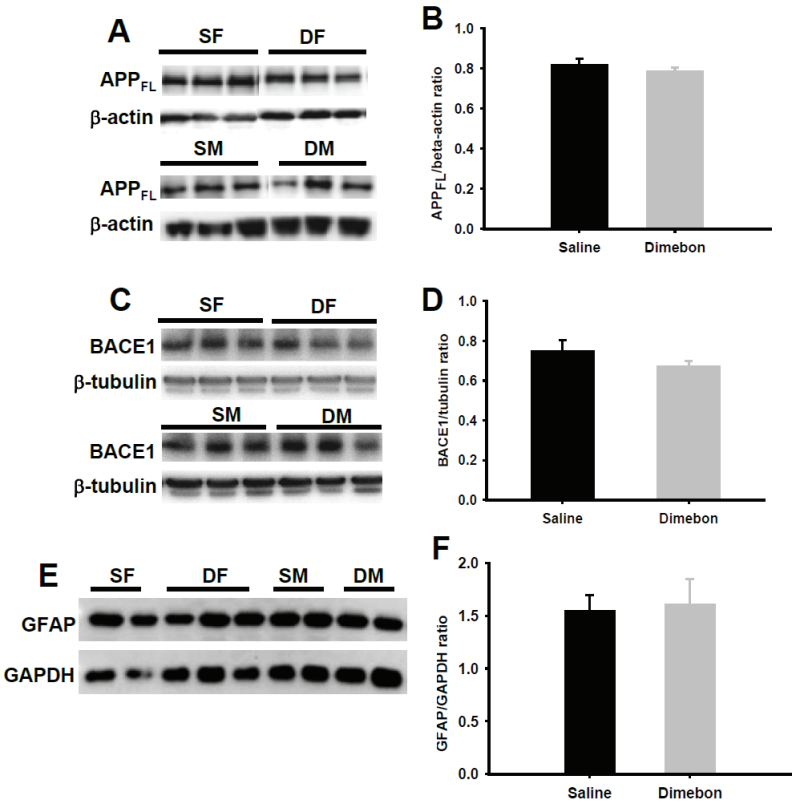

Figure 3. Representative immunoblots for APP full length (FL) (A), BACE1 (C) and GFAP (E) and respective histograms (B, D, F) showing no significant differences in soluble protein levels between dimebon and saline-treated 3xTg-AD mice. Abbreviations: SF, saline-treated females, SM, saline-treated males, DF, dimebon-treated females, DM, dimebon-treated males.

ture was measured 1, 2 and 3 days post dimebon treatment (**Figure 5C-I**). After 1 day of treatment there were no significant changes in the intensity of GFAP immunolabeling between the controls at any dimebon concentration (**Figure 5I**; p=0.087). By contrast, astrocyte cultures treated with 50 μM concentration of dimebon for 2 and 3 days showed a significant increase in GFAP immunofluorescence compared to cultures containing 10 μM dimebon and controls (no dimebon) (**Figure 5C-I**; Kruskal-Wallis on ranks p<0.001).

Discussion

Dimebon, Aβ and tau pathology in the hippocampus of 3xTg-AD mice

In the present study, we evaluated the effects of dimebon, a controversial therapeutic drug for the treatment of AD, upon Aβ and tau pathology in the hippocampus of the 3xTg-AD mouse [9, 10]. At age 6.5 months, prior to the development of Aβ plaques in the hippocampus of male and female 3xTg-AD mice [11], mice received a daily i.p. injection of 0.1 % dimebon or saline for 1.5 months. At 8 months of age and after the last injection LC-MS/MS analysis revealed that dimebon reached the brain and that drug treated mice displayed larger concentrations of a molecule with a mass similar to that identified as dimebon [7, 17, 28].

Neuropathological evaluation revealed a select reduction in APP/Aβ immunoreactivity within the entire hippocampus including CA1 neurons and subiculum in dimebon compared to saline-treated 3xTg-AD mice. In addition, there was a negative correlation between APP/Aβ positive OD measurements in the subiculum and dimebon levels, suggesting a possible drug effect on amyloid metabolism. While the levels of soluble $A\beta_{1\text{-}42}/A\beta_{1\text{-}40}$, oligomeric Aβ, full length APP, and BACE1 were unchanged in dimebon-treated 3xTg-AD mice, we observed a trend for an increase in insoluble Aβ plaques in the hippocampus of dimebon-treated mutant mice. Therefore, it is possible that dimebon accelerates the deposition of insoluble Aβ into plaques without changing the levels of soluble Aβ species. In this regard, acute doses of dimebon increase extracellular Aβ levels in *in vivo* and *in vitro* models of AD [29]. By contrast, an *in vitro* study did not reveal changes in total Aβ levels ($A\beta_{1\text{-}40}$ and $A\beta_{1\text{-}42}$) and soluble oligomeric Aβ species after 4 months of chronic dimebon treatment in TgCRND8 AD mice, suggesting that dimebon does not modify the production of Aβ [7]. These contradictory findings indicate the need to investigate whether dimebon activates or regulates mechanisms that clear insoluble Aβ species by accelerating their aggregation into larger Aβ clusters/plaques, without changing Aβ

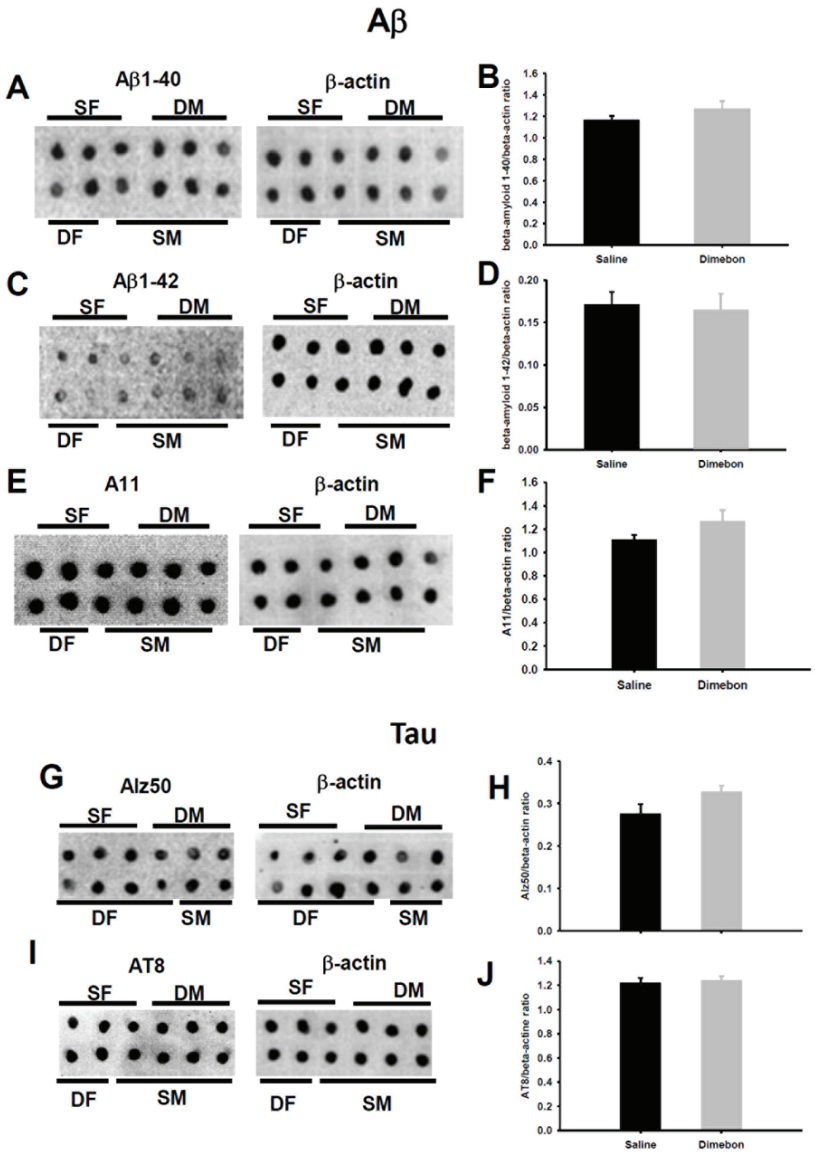

Figure 4. Representative dot blots for $A\beta_{1-40}$ (A), $A\beta_{1-42}$ (C), A11 (E), Alz50 (G) and AT8 (I) and histograms (B, D, F, H, J) showing no significant differences in soluble protein levels between dimebon and saline-treated 3xTg-AD mice. Abbreviations: SF, saline-treated females, SM, saline-treated males, DF, dimebon treated females, DM, dimebon-treated males.

production.

Interestingly, we found that Alz50-ir OD measurements, an early conformational tau marker, have a tendency to decrease in the CA1 hippocampal pyramidal cells in dimebon-treated mice. Our dot blot data revealed no difference either for Alz50 or AT8 tau levels between dimebon treated and non-treated groups. These results indicated that tau is not significantly affected by dimebon and the trend towards a decrease may reflect a reduction in APP/Aβ since tau has been considered a secondary event to Aβ pathology in these mice [10]. However more studies are needed to determine whether dimebon could affect tau pathology in AD.

Dimebon protects against Aβ toxicity and inflammation

The present *in vitro* experiments demonstrated that dimebon has neuroprotective properties against Aβ toxicity. Specifically, we showed the viability of human neuroblastoma cells (SH-SY5Y) exposed to 25μM and 50μM dimebon and challenged with 10 μM $A\beta_{1-42}$ or $A\beta_{25-35}$ was significantly increased when compared with neuronal cultures exposed to Aβ alone. Similar results were reported using primary cerebellar granule cell cultures, where 25 μM dimebon increased the viability of the cerebellar neurons treated with $A\beta_{25-35}$ [1]. In addition, 50 μM dimebon protected primary cultures of striatal medium spiny neurons harvested from YAC128 HD transgenic mice from glutamate-induced apoptosis and stabilized glutamate-induced Ca^{2+} signals [28]. Together these observations suggest that dimebon in high concentrations stimulates neuronal survival and/or inhibits apoptotic pathways *in vitro* when exposed to neurotoxins such as Aβ or glutamate. Since Aβ also destabilizes mitochondrial pore permeability and Ca^{2+} concentrations, it is possible that dimebon alters the affect of Aβ on these cell death pathways, as well [30]. Notably, several *in*

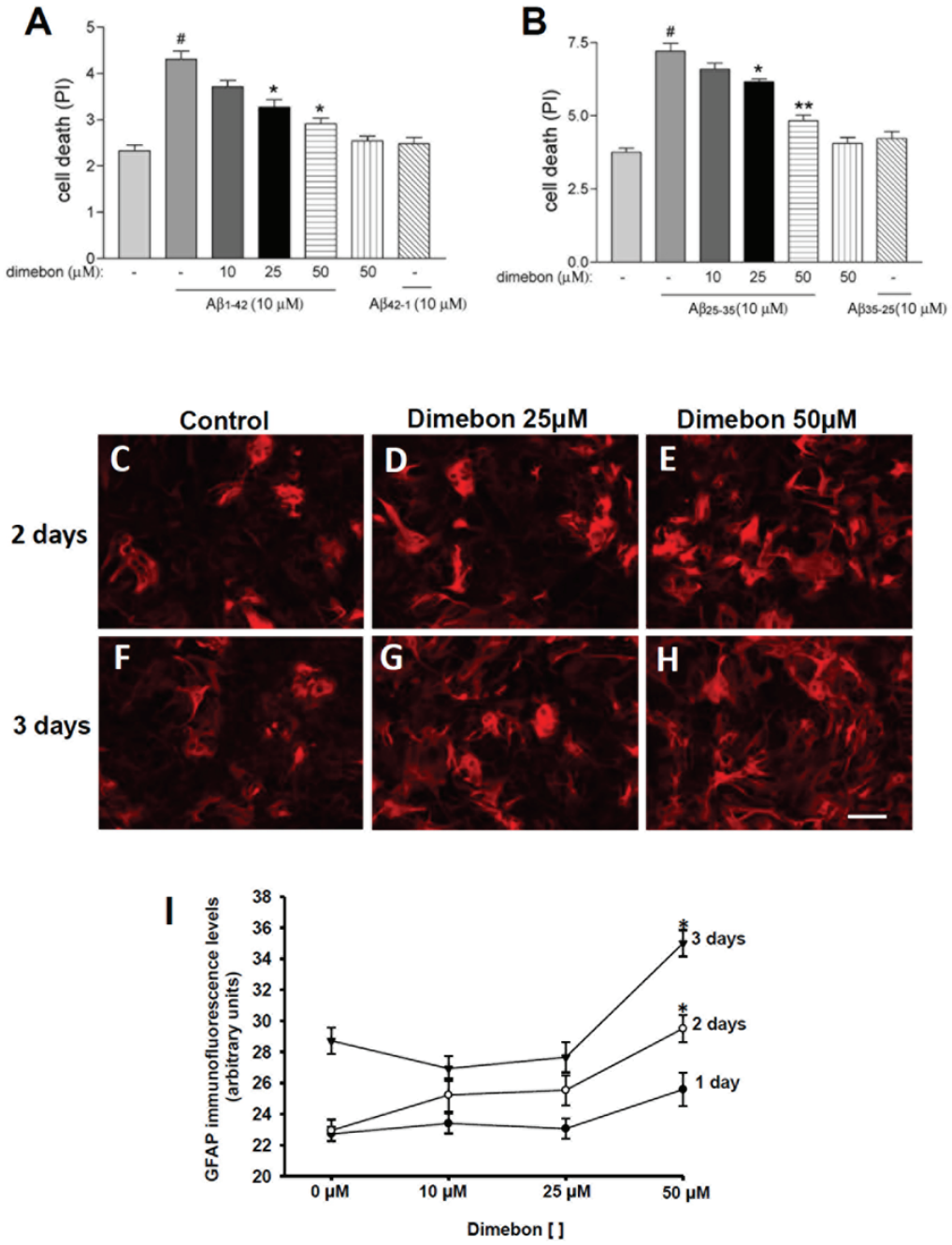

Figure 5. SH-SY5Y neuronal cultures were stained with propidium iodide (PI) after dimebon, $A\beta_{1\text{-}42}$ (A) or $A\beta_{1\text{-}35}$ (B) challenge to evaluate the neuronal protective effects of dimebon against Aβ toxicity. Statistical evaluation of SH-SY5Y neuronal cultures stained with PI revealed a significant increase in cell viability in SH-SY5Y neuronal cultures loaded with 25μM and 50μM dimebon and challenged with 10 μM $A\beta_{1\text{-}42}$ or $A\beta_{25\text{-}35}$ compared to those treated only with 10 μM $A\beta_{1\text{-}42}$. Neuronal mortality was significantly increased in cell cultures loaded with $A\beta_{1\text{-}42}$ or $A\beta_{25\text{-}35}$ compared to control. There was no statistical difference between controls and cell cultures loaded with reverse peptides $A\beta_{25\text{-}35}$ with or without dimebon (*p<0.01 and **p<0.001for $A\beta_{25\text{-}35}$; *p<0.001 for $A\beta_{1\text{-}42}$ #p<0.001). (C-H) Images of mouse primary astrocyte cultures showing an increase in GFAP immunoreactivity in cultures treated with 50 μM dimebon for 2 (E) and 3 (H) days. (I) Statistical analysis confirmed that GFAP immunoreactivity was significantly increased in cultures treated with 50 μM for 3 days compared to cultures without dimebon or containing 10 μM and 25 μM dimebon, whereas after two days GFAP immunoreactiviy was significantly increased compared to 10 μM and control cultures. (*p < 0.001). Scale bar=100.

vitro studies demonstrate that dimebon improves mitochondrial function in the face of pathological stressors such as Aβ [31-33]. These findings indicate the neuroprotective effects of dimebon are associated with preservation/enhancing mitochondrial function and, thus cell survival in pathological and non-pathological conditions. On the other hand, amyloid transgenic CRND8 mice chronically treated with dimebon failed to show an improvement in mitochondrial function [7]. Dimebon may have multiple effects as it also interacts with a broad spectrum of biological targets (NMDA receptors, Ca^{2+} channels), and antagonizes alpha-adrenergic, histamine H1 and H2, and serotonin receptors with high affinity [1, 28, 34]. Therefore, despite our results, which extend and support previous findings, the exact mechanism(s) of action underlying the neuroprotective effects of dimebon remain to be clarified.

Here, we report for the first time that dimebon stimulates the production of the cytoskeleton intermediate filament GFAP in mouse primary astrocyte cultures. Mouse astrocyte cultures exposed to the highest concentration of dimebon (50 μm) displayed an 18% increment in GFAP levels compared to control astrocyte cultures without drug treatment. At present the mechanisms of action involved in the stimulation of GFAP expression in mouse cultured astrocytes by dimebon are unknown. Dimebon has been characterized as a non-selective antihistamine and proven to mediate this effect by blocking H1-histamine receptors [35]. This receptor is present in astrocytes and is involved in the histamine-signaling pathway responsible for NGF synthesis, a neurotrophic factor that promotes cell survival [36]. Moreover, dimebon also binds with high affinity to several serotoninergic receptors [28, 37], in particular 5-HT5A receptors, which are expressed in astrocytes [38]. It is well known that astrocytes play a pivotal role in brain homeostasis, and together with microglia are the cellular elements involved in neuroinflammation, a defense mechanism, which protect neurons against brain insult [39]. Enlargement of astrocytes and increased expression of GFAP is an indication of reactive astrocytes (gliosis) in response to brain damage. In addition, astrocytes display large amounts of Aβ, suggesting that they play a role in Aβ clearance [40]. We suggest that dimebon promotes a mechanism of neuroprotection against Aβ and other insults via astrocytic stimulation. On the other hand, chronic activation of astrocytes could have a detrimental role in the development of AD via the overexpression of the proinflammatory cytokine interleukin 1 (IL-1), which can induce plaque formation [41-43] and lead to neuronal death rather than protection [44]. Future studies are needed to explore the potential effects of dimebon upon neuroinflammation in AD.

In summary, the present investigation indicates that chronic dimebon treatment significantly reduces intracellular APP/Aβ in the hippocampus of both male and female treated compared to control 3xTg-AD mice. These changes in APP/Aβ were not accompanied by changes in tau pathology in dimebon treated mice. Likewise, *in vitro* acute dimebon treatment protected SH-SY5Y cells against Aβ toxicity and promoted GFAP expression of mouse primary astrocyte cultures. These data demonstrate that dimebon may protect neurons by a dual process of modifying Aβ pathology and stimulating astrocytosis in AD.

Acknowledgments

Supported by RO1AG10688 (EJM), R01AG030142 (RV), R01AG022560 (RV), F32AG033445 (KS) and the Shapiro Foundation (EJM).

Address correspondence to: Dr. Sylvia E Perez, Department of Neurological Sciences, Rush University Medical Center, 1735 W. Harrison Street, Suite 324, Chicago, IL 60612, USA. Tel: 312-563-3580; Fax: 312-563-3571; E-mail: Sylvia_e_perez@rush.edu

References

[1] Bachurin S, Bukatina E, Lermontova N, Tkachenko S, Afanasiev A, Grigoriev V, Grigorieva I, Ivanov Y, Sablin S and Zefirov N. Antihistamine agent Dimebon as a novel neuroprotector and a cognition enhancer. Ann N Y Acad Sci 2001; 939: 425-435.

[2] Doody RS, Gavrilova SI, Sano M, Thomas RG, Aisen PS, Bachurin SO, Seely L, Hung D and dimebon investigators. Effect of dimebon on cognition, activities of daily living, behaviour, and global function in patients with mild-to-moderate Alzheimer's disease: a randomised, double-blind, placebo-controlled study. Lancet 2008; 372: 207-215.

[3] Kieburtz K, McDermott MP, Voss TS, Corey-Bloom J, Deuel LM, Dorsey ER, Factor S, Geschwind MD, Hodgeman K, Kayson E, Noonberg S, Pourfar M, Rabinowitz K, Ravina B, Sanchez-

Ramos J, Seely L, Walker F, Feigin A and Huntington Disease Study Group DIMOND Investigators. A randomized, placebo-controlled trial of latrepirdine in Huntington disease. Arch Neurol 2010; 67: 154-160.

[4] Pfizer Press Release (2010). Pfizer and Medivation announce results from two phase 3 studies in Dimebon (latrepirdine*) Alzeimer's disease clinical development program Obtained from http://investors.medivation.com/releasedetail.cfm?release ID=448818.

[5] Lermontova NN, Lukoyanov NV, Serkova TP, Lukoyanova EA and Bachurin SO. Dimebon improves learning in animals with experimental Alzheimer's disease. Bull Exp Biol Med 2000; 129: 544-546.

[6] Vignisse J, Steinbusch HW, Bolkunov A, Nunes J, Santos AI, Grandfils C, Bachurin S and Strekalova T. Dimebon enhances hippocampus-dependent learning in both appetitive and inhibitory memory tasks in mice. Prog Neuropsychopharmacol Biol Psychiatry 2011; 35: 510-522.

[7] Wang J, Ferruzzi MG, Varghese M, Qian X, Cheng A, Xie M, Zhao W, Ho L and Pasinetti GM. Preclinical study of dimebon on β-amyloid-mediated neuropathology in Alzheimer's disease. Mol Neurodegener 2011; 6: 7.

[8] Webster SJ, Wilson CA, Lee CH, Mohler EG, Terry AV Jr and Buccafusco JJ. The acute effects of dimebolin, a potential Alzheimer's disease treatment, on working memory in rhesus monkeys. Br J Pharmacol 2011; 164: 970-978.

[9] Oddo S, Caccamo A, Shepherd JD, Murphy MP, Golde TE, Kayed R, Metherate R, Mattson MP, Akbari Y and LaFerla FM. Triple-transgenic model of Alzheimer's disease with plaques and tangles: intracellular Abeta and synaptic dysfunction. Neuron 2003; 39: 409-421.

[10] Oddo S, Caccamo A, Kitazawa M, Tseng BP and LaFerla FM. Amyloid deposition precedes tangle formation in a triple transgenic model of Alzheimer's disease. Neurobiol Aging 2003; 24: 1063-1070.

[11] Oh KJ, Perez SE, Lagalwar S, Vana L, Binder L and Mufson EJ. Staging of Alzheimer's pathology in triple transgenic mice: a light and electron microscopic analysis. Int J Alzheimers Dis 2010; pii: 780102.

[12] Braak H and Braak E. Neuropathological stageing of Alzheimer-related changes. Acta Neuropathol 1991; 82: 239-259.

[13] Braak H and Braak E. Demonstration of amyloid deposits and neurofibrillary changes in whole brain sections. Brain Pathol 1991; 1: 213-216.

[14] Thal DR, Rüb U, Orantes M and Braak H. Phases of A beta-deposition in the human brain and its relevance for the development of AD. Neurology 2002; 58: 1791-1800.

[15] Muramori F, Kobayashi K and Nakamura I. A quantitative study of neurofibrillary tangles, senile plaques and astrocytes in the hippocampal subdivisions and entorhinal cortex in Alzheimer's disease, normal controls and non-Alzheimer neuropsychiatric diseases. Psychiatry Clin Neurosci 1998; 52: 593-599.

[16] Perez SE, He B, Muhammad N, Oh K-J, Fahnestock M, Ikonomovic M and Mufson EJ. Cholinotrophic basal forebrain system alterations in 3xTg-AD transgenic mice. Neurobiol Dis 2011; 41: 338-352.

[17] Nirogi R, Kandikere V, Mudigonda K, Komarneni P and Boggavarapu R. Liquid chromatography-tandem mass spectrometry method for the quantification of dimebon in rat plasma and brain tissue. J Chromatogr B Analyt Technol Biomed Life Sci 2009; 877: 3563-3571.

[18] Mufson EJ, Lavine N, Jaffar S, Kordower JH, Quirion R and Saragovi HU. Reduction in p140-TrkA receptor protein within the nucleus basalis and cortex in Alzheimer's disease. Exp Neurol 1997; 146: 91-103.

[19] Perez SE, Lazarov O, Koprich JB, Chen EY, Rodriguez-Menendez V, Lipton JW, Sisodia SS and Mufson EJ. Nigrostriatal dysfunction in familial Alzheimer's disease-linked APPswe/PS1DeltaE9 transgenic mice. J Neurosci 2005; 25: 10220-10229.

[20] Moeller ML and Dimitrijevich SD. A new strategy for analysis of phenotype marker antigens in hollow neurospheres. J Neurosci Methods 2004; 139: 43-50.

[21] Giuffrida ML, Grasso G, Ruvo M, Pedone C, Saporito A, Marasco D, Pignataro B, Cascio C, Copani A and Rizzarelli E. Abeta(25-35) and its C- and/or N-blocked derivatives: copper driven structural features and neurotoxicity. J Neurosci Res 2007; 85: 623-633.

[22] Millucci L, Ghezzi L, Bernardini G and Santucci A. Conformations and biological activities of Amyloid Beta Peptide 25-35. Curr Protein Pept Sci 2009; 11: 54-67.

[23] Walsh DM, Hartley DM, Kusumoto Y, Fezoui Y, Condron MM, Lomakin A, Benedek G B, Selkoe DJ and Teplow DB. Amyloid beta-protein fibrillogenesis. Structure and biological activity of protofibrillar intermediates. J Biol Chem 1999; 274: 25945-25952.

[24] Chromy BA, Nowak RJ, Lambert MP, Viola KL, Chang L, Velasco PT, Jones BW, Fernandez SJ, Lacor PN, Horowitz P, Finch CE, Krafft GA and Klein WL. Self-assembly of Abeta(1-42) into globular neurotoxins. Biochemistry 2003; 42: 12749-12760.

[25] Counts SE and Mufson EJ. Noradrenaline activation of neurotrophic pathways protects against neuronal amyloid toxicity. J Neurochem 2010; 113: 649-660.

[26] Guilian D and Baker TJ. Characterization of ameboid microglia isolated from developing mammalian brain. J Neurosci 1986; 6: 2163-2178.

[27] Pahan K, Liu X, McKinney MJ, Wood C, Sheikh

FG and Raymond JR. Expression of a dominant-negative mutant of p21(ras) inhibits induction of nitric oxide synthase and activation of nuclear factor-kappaB in primary astrocytes. J Neurochem 2000; 74: 2288-2295.
[28] Wu J, Li Q and Bezprozvanny I. Evaluation of Dimebon in cellular model of Huntington's disease. Mol Neurodegener 2008; 21: 3-15.
[29] Steele JW, Kim SH, Cirrito JR, Verges DK, Restivo JL, Westaway D, Fraser P, St George Hyslop P, Sano M, Bezprozvanny I, Ehrlich ME, Holtzman DM and Gandy S. Acute dosing of latrepirdine (DimebonTM), a possible Alzheimer therapeutic, elevates extracellular amyloid-beta levels in vitro and in vivo. Mol Neurodegener 2009; 17: 51.
[30] Giorgi C, Baldassari F, Bononi A, Bonora M, De Marchi E, Marchi S, Missiroli S, Patergnani S, Rimessi A, Suski JM, Wieckowski MR and Pinton P. Mitochondrial Ca(2+) and apoptosis. Cell Calcium 2012; 52: 36-43.
[31] Bachurin SO, Shevtsova EP, Kireeva EG, Oxenkrug GF and Sablin SO. Mitochondria as a target for neurotoxins and neuroprotective agents. Ann N Y Acad Sci 2003; 993: 334-344.
[32] Zhang S, Hedskog L, Petersen CA, Winblad B and Ankarcrona M. Dimebon (latrepirdine) enhances mitochondrial function and protects neuronal cells from death. J Alzheimers Dis 2010; 21: 389-402.
[33] Eckert SH, Eckmann J, Renner K, Eckert GP, Leuner K and Muller WE. Dimebon Ameliorates Amyloid-β Induced Impairments of Mitochondrial Form and Function. J Alzheimers Dis 2012; 31: 21-32.
[34] Grigorev VV, Dranyi OA, Bachurin SO. Comparative study of action mechanisms of dimebon and memantine on AMPA- and NMDA-subtypes glutamate receptors in rat cerebral neurons. Bull Exp Biol Med 2003; 136: 474-477.
[35] Matveeva IA. Action of dimebon on histamine receptors. Farmakol Toksikol 1983; 46: 27-29.
[36] Lipnik-Stangelj M. Multiple role of histamine H1 -receptor-PKC-MAPK signalling pathway in histamine-stimulated nerve growth factor synthesis and secretion. Biochem Pharmacol 2006; 72: 1375-1381.
[37] Schaffhauser H, Mathiasen JR, Dicamillo A, Huffman MJ, Lu LD, McKenna BA, Qian J and Marino MJ. Dimebolin is a 5-HT(6) antagonist with acute cognition enhancing activities. Biochem Pharmacol 2009; 78: 1035-1042.
[38] Carson MJ, Thomas EA, Danielson PE and Sutcliffe JG. The 5HT5A serotonin receptor is expressed predominantly by astrocytes in which it inhibits cAMP accumulation: a mechanism for neuronal suppression of reactive astrocytes. Glia 1996; 17: 317-326.
[39] Allaman I, Bélanger M and Magistretti PJ. Astrocyte-neuron metabolic relationships: for better and for worse. Trends Neurosci 2011; 34: 76-87.
[40] Nagele RG, D'Andrea MR, Lee H, Venkataraman V and Wang HY. Astrocytes accumulate A beta 42 and give rise to astrocytic amyloid plaques in Alzheimer disease brains. Brain Res 2003; 971: 197-209
[41] Goldgaber D, Harris HW, Hla T, Maciag T, Donnelly RJ, Jacobsen JS, Vitek MP and Gajdusek DC. Interleukin 1 regulates synthesis of amyloid beta-protein precursor mRNA in human endothelial cells. Proc Natl Acad Sci USA 1989; 86: 7606-7610.
[42] Griffin WS, Stanley LC, Ling C, White L, MacLeod V, Perrot LJ, White CL 3rd and Araoz C. Brain interleukin 1 and S-100 immunoreactivity are elevated in Down syndrome and Alzheimer disease. Proc Natl Acad Sci USA 1989; 86: 7611-7615.
[43] Li Y, Liu L, Barger SW and Griffin WS. Interleukin-1 mediates pathological effects of microglia on tau phosphorylation and on synaptophysin synthesis in cortical neurons through a p38-MAPK pathway. J Neurosci 2003; 23: 1605-1611.
[44] Griffin WS. Alzheimer's - Looking beyond plaques. F1000 Med Rep 2011; 3: 24.